IEEE Access
Multidisciplinary | Rapid Review | Open Access Journal

SPECIAL SECTION ON KEY ENABLING TECHNOLOGIES FOR PROSUMER ENERGY MANAGEMENT

Received October 5, 2020, accepted October 12, 2020, date of publication October 16, 2020, date of current version October 28, 2020.

Digital Object Identifier 10.1109/ACCESS.2020.3031720

Characteristics Analysis of Inertia Damping of Grid-Connected System of Direct-Drive Wind Power Generation

SHENGQING LI, YU JIANG, BALING FANG, (Member, IEEE), AND CHENYANG WANG

School of Electrical and Information Engineering, Hunan University of Technology, Zhuzhou 412007, China
Photovoltaic Micro-grid Intelligent Control Technology Hunan Engineering Research Center, Zhuzhou 412007, China

Corresponding author: Baling Fang (5911866@qq.com)

This work was supported in part by the National Natural Science Foundation of China under Grant 51977072, in part by the National Research and Development Program under Grant 2018YFB0606005, in part by the Hunan Natural Science Foundation under Grant 2017JJ4024, and in part by the General Project of Hunan Provincial Education Department under Grant 18C0502.

ABSTRACT As large-scale direct-drive wind turbine generator set is connected to the grid, the power system will face problems such as reduced inertia and insufficient frequency modulation capability. The control of wind turbine virtual inertia is an important way to solve this problem. Therefore, this paper takes the direct-drive wind power generation system as the research object, draws lessons from the multi-time scale modeling idea, and based on the electrical torque analysis, establishes the DC voltage time model with the wind turbine virtual inertia control. Based on this, inertia damping characteristics of direct-drive wind power grid-connected system are analyzed. The results show that the dynamic characteristic parameters of the system are affected by many factors, among which the equivalent inertia coefficient of the system is mainly affected by DC capacitance, DC bus voltage and wind turbine virtual inertia control parameters. Damping coefficient is mainly affected by steady-state operating point and DC voltage proportional control parameter K_{pu}. The synchronization coefficient is mainly affected by steady-state operating point and DC voltage integration control parameter K_{iu}. The correctness of mechanism analysis of inertia damping characteristics of the whole system is verified by simulation, which provides a certain theoretical reference for inertia damping research of electronic power system.

INDEX TERMS Direct-drive wind power, multiple-time scale, inertia damping characteristics, power electronics dominated power systems.

I. INTRODUCTION

Direct-driven Wind Turbine with Permanent-Magnet Synchronous Generator (D-PMSG) has been widely used in wind power grid connection due to its advantages of small size and low operating cost [1], [2]. Considering the power converter control based D-PMSG, the power control is decoupled from the grid frequency response [3], the wind turbine cannot participate in the grid frequency response under the control of Maximum Power Point Tracking (MPPT). However, large-scale ventilators are connected to the grid through power electronic devices. Therefore, the power system is gradually developing towards the orientation of power electronics [4]. The inertia and damping of traditional systems based on thermal and hydropower may gradually weaken, thereby threatening the stability of a power system [31].

At present, many literatures are focused on the wind turbines frequency adjustment strategy. The Virtual Synchronous Generator (VSG) control is used to provide inertia characteristics for grid-connected inverter and it has become a research hotspot [30]. The VSG control energy storage is required to provide inertia without the economy advantage and does not take advantage of fast response power electronic devices. In a wind farm, the D-PMSG inertia time constant of megawatt level is generally 2∼6s [8], [9]. When the wind turbine is in normal operation, the stored rotor kinetic energy of the unit is considerable [10]. In order to make use of the kinetic energy of the wind turbine rotor, based on the MPPT control [8], [9], the auxiliary power instruction P_{VIC} is generated to minimize the frequency deviation by PD controlling. So as to mobilize the kinetic energy of the wind turbine

The associate editor coordinating the review of this manuscript and approving it for publication was Bin Zhou.

rotor to respond to the frequency change of the power grid and provide inertia support for the system. In [10], a virtual inertia coordinated control strategy for weak-grid is proposed based on the dynamic characteristics of DC voltage. The above literatures of the inertia characteristics of wind power generation system are only focused on the inertia control of the equipment itself. On the one hand, the dynamic process under DC capacity control of grid-connected inverter is not considered, and on the other hand, the dynamic stability of the grid-connected wind power generation system is not studied. In [11], [12], the method of simulating the generator rotor motion process with DC side capacitance is proposed, and it can also provide certain inertia characteristics for the system. In [13], the inertia characteristics and the influencing factors of the DC side capacitance of grid-connected inverter are studied. In [14], [15], the inertia damping characteristics of the system are studied based on the electrical torque method without considering the dynamic characteristics of the new energy units.

In order to analyze the dynamic characteristics of wind generation system, the idea of a multiple time scale analysis is put forward in [16], [17]. According to the characteristics of power electronic system of wind power generation, the time scale is divided. In [18], based on the idea of multiple time scale division, the influence of the reactive power control of grid connected inverter on the dynamic characteristics of the system is studied. In order to study the dynamic stability of the DC voltage time scale, the doubly-fed wind turbine was analyzed in [19], [20]. The above literature analysis focuses on the research of converter control, and does not fully consider the effect of electromechanical time scale on the later DC voltage time scale, so the general conclusion can not be obtained. However, the study of converter control has not fully taken into account the effect of electromechanical time scale on the later DC voltage time scale, so the general conclusion can not be obtained. In a word, the idea of multiple time scale analysis provides a new analytical thinking to study the dynamic stability of power electronic system.

Based on the above research, this paper takes the direct-drive wind power grid-connected system as the research object. Based on the idea of multi-time scale analysis, the equivalent inertia damping characteristics of the system with wind turbine virtual inertia are studied by using electrical torque method under the control of DC voltage time scale, and the law that influences the equivalent parameters of the system is analyzed. The correctness of the analysis of the system inertia damping characteristics is verified by simulation analysis, which provides theoretical basis for inertia damping parameter design of wind power generation system.

II. TOPOLOGY AND CONTROL OF D-PMSG GRID CONNECTED SYSTEM

The topology structure and control block diagram of D-PMSG grid-connected system is shown in Fig. 1. In this figure, D-PMSG is connected to the power grid through a power converter. The machine-side converter controls

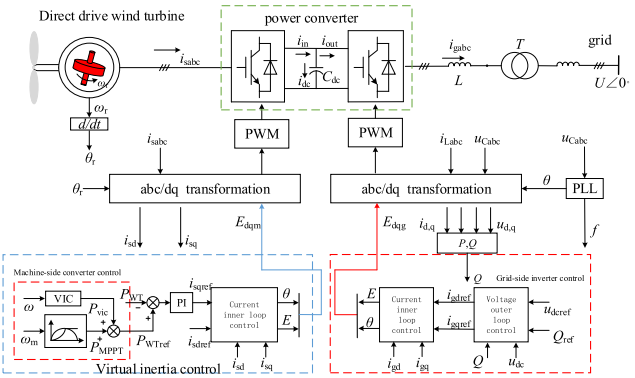

FIGURE 1. Topology and control block diagram of the grid connected system of D-PMSG.

the wind turbines output power and realizes MPPT control and the grid-side inverter realizes stable control of DC voltage.

In this figure, P_{WTref} is the rated power of the wind turbine output (including the maximum tracking power P_{MPPT} and the virtual inertia power P_{vic}), ω_{r} is the wind turbine frequency, rotation speed i_{sabc} is the stator current of the generator, u_{dc} is the DC bus voltage, C_{dc} is the DC bus capacitance, and L is the filter inductance.

A. VIRTUAL INERTIA CONTROL OF MACHINE SIDE CONVERTER

As shown in Fig. 1, the machine-side converter control, in order to make the wind turbine rotor participate in the frequency response of the grid, a virtual inertia is added to the direct power control. The differential controller is used to introduce the variation signal of grid frequency into the power control so that the ventilator power is coupled to the grid frequency [28]. The equation of virtual inertia control can be written as

$$P_{\mathrm{WTref}} = P_{\mathrm{MPPT}} + P_{\mathrm{vic}} = P_{\mathrm{MPPT}} + K_{\mathrm{v}} df/\mathrm{dt} \qquad (1)$$

where P_{WTref} is the rated active power of the ventilator, P_{MPPT} is the maximum tracking power of the ventilator, P_{vic} is the virtual inertia control output auxiliary power, K_{v} is the virtual inertia control coefficient, and f is the grid-frequency. Vector control of stator current orientation and grid voltage orientation is used in machine-side control and grid-side control respectively, while stator current and grid-connected current are used in inner ring for control respectively.

Formula (1) shows that when the wind turbine is running in the MPPT control mode, the wind turbine is decoupled from the grid frequency, namely $P_{\mathrm{WTref}} = P_{\mathrm{MPPT}}$, and the rotor kinetic energy cannot respond to the grid frequency change. When the virtual inertia control is used, the variation of the grid frequency will form the virtual inertia command P_{vic}. Meanwhile, this equation can be expressed as $P_{\mathrm{WTref}} = P_{\mathrm{MPPT}} + P_{\mathrm{vic}}$, and the rotor loses part of the rotor kinetic energy to provide frequency of support for the grid.

B. DC CAPACITOR VOLTAGE CONTROL OF THE GRID-SIDE INVERTER

As shown in Fig. 1, so as to maintain the stability of the inverter DC bus, the grid-side inverter takes voltage and current double closed-loop domination. Compared with the DC voltage time scale of the voltage outer loop, the AC current time scale of the current inner loop can be ignored in dynamic analysis [14], and the inverter output current can be described as

$$i_s = i_d = (u_{dc} - U_{dcref})(K_{pu} + K_{iu}/s) \tag{2}$$

where i_d is the d-axis component of the grid-connected current when the grid-connected inverter is oriented according to the grid voltage vector, K_{pu} and K_{iu} are respectively the proportional control coefficient and integral control coefficient in the outer voltage loop PI-controller.

III. THE ANALYSIS OF INERTIA DAMPING CHARACTERISTICS OF D-PMSG GRID-CONNECTED SYSTEM

In the analysis of static stability and dynamic instability mechanism of synchronous power system, the incremental equation of generator is usually used [26]. It is expressed as

$$\begin{cases} \dfrac{d\Delta\delta}{dt} = \Delta\omega \\ 2H_{sg}\dfrac{d\Delta\omega}{dt} = \Delta P_{in} - \Delta P_{out} - D\Delta\omega \end{cases} \tag{3}$$

where $\Delta\delta$ is the power angle variation of the generator system, H_{sg} is the inertia time constant of the generator, ΔP_{in} and ΔP_{out} are variations of input and output power of the generator respectively, and D is the damping coefficient of the generator system. Referring to the dynamic characteristic analysis principle of generator, the dynamic process of wind turbine and DC capacitor is analyzed in detail below.

A. DYNAMIC CHARACTERISTICS OF WIND IN ANSWER TO GRID FREQUENCY

When the wind is running normally, the motion equation of the generator rotor can be written as

$$J_{WT}\omega_r\frac{d\omega_r}{dt} = P_m - P_e \tag{4}$$

where J_{WT} is the inherent moment of inertia of the wind turbine and ω_r is the rotational speed of the wind turbine rotor. P_m and P_e are the wind turbine input mechanical power and output electromagnetic power respectively. Permanent magnet generator is similar to conventional synchronous generator. When the rotor loss is set aside, the kinetic energy reserved by the mechanical rotor can be written as [28]

$$E_k = \int J_{WT}\omega_r d\omega_r = \frac{1}{2}J_{WT}\omega_r^2 = \frac{1}{2p^2}J_{WT}\omega_{er}^2 \tag{5}$$

where p is the polar number of the generator and ω_{er} is the electrical angular velocity of the wind turbines. When the ventilator responds to frequent change of the system, variation of rotor kinetic energy is expressed as

$$\begin{aligned} \Delta E_k &= \frac{1}{2p^2}J_{WT}\left[(\omega_{er0} + \Delta\omega_{er})^2 - \omega_{er0}^2\right] \\ &\approx \omega_{er0}\frac{J_{WT}}{p^2}\Delta\omega_{er} \end{aligned} \tag{6}$$

where ω_{er0} is the initial angular velocity of the wind turbine and $\Delta\omega_{er}$ is variation of the wind-driven machine palstance. To facilitate analysis, formula (6) can be expressed as

$$\begin{aligned} \Delta E_k^* &= \frac{\Delta E_k}{S_B} = \frac{2\,J_{WT}\omega_{er0}^2}{2\,S_B p^2}\frac{\Delta\omega_{er}}{\omega_{er0}} \\ &= \frac{2\,H_{WT}}{p^2}\frac{\Delta\omega_{er}}{\omega_{er0}} \end{aligned} \tag{7}$$

where S_B means the rated capacity of the system and H_{WT} is the inertia time constant of the ventilator. Under the control of virtual inertia regulation, the kinetic energy released by the rotor and the energy of the auxiliary inertia are equal [8]. So it can be written as $dE_k/dt = P_{vic}$. When variations of the system frequency are little, it can be obtained as

$$\begin{aligned} dE_k/dt = P_{vic} &\Rightarrow \frac{2\,H_{WT}}{p^2}\frac{\Delta\omega_{er}}{\omega_{er0}} = \frac{K_v\Delta\omega}{2\pi\omega_0} \\ &\Rightarrow K_v = \frac{4\pi H_{WT}}{p^2}k_\omega \end{aligned} \tag{8}$$

where $\Delta\omega$ is the change of grid synchronous angular frequency, ω_0 is the grid synchronous angular frequency, k_ω is the virtual inertia adjustment depth, it can be obtained as

$$k_\omega = \frac{\Delta\omega_{er}/\omega_{er0}}{\Delta\omega/\omega_0} \tag{9}$$

Equation (7) shows the dynamic characteristics of the wind turbine under the virtual inertia control. Equation (8) shows that under the control of virtual inertia, the contribution of ventilator rotor to frequency response of grid is not only related to the inertia of the ventilator itself, but also related to the modulation depth k_ω.

B. DYNAMIC MODEL UNDER DC VOLTAGE TIME SCALE OF DC CAPACITOR ON GRID SIDE

The direct-current capacitance of grid side inverter, as the energy storage power electronic equipment in the system, connects the wind turbine side converter and grid connected inverter. Its dynamic characteristics reflect the equilibrium state of input and output energy. As shown in Fig.2, it is the schematic diagram of capacitor charging and discharging. The process of capacitor charging and discharging can be described as follows

$$i_c = C_{dc}\frac{du_{dc}}{dt} = i_{dc} - i_s \tag{10}$$

where C_{dc} is DC side capacitance, I_{dc} is DC side input current (output current of generator side converter), and i_s is current injected into grid side inverter.

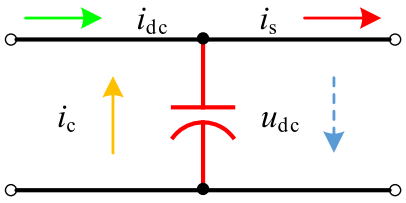

FIGURE 2. Capacitor charging and discharging diagram.

Considering the balance of input and output power, equation (10) can be converted into power expression, and normalization (voltage reference selects DC bus voltage U_{dc}, and power selection system rated capacity S_B) can be obtained as [14]

$$\frac{C_{dc}U_{dc}^2}{S_B}\frac{du_{dc}}{dt} = P_{dc} - P_s \tag{11}$$

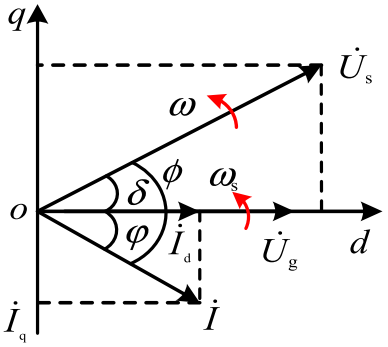

FIGURE 3. Voltage and current vector.

According to Fig. 3, the vector diagram of grid-connected current control when the grid voltage is oriented. According to the figure, the grid-connected current can be expressed as (ignoring the filter capacitive current component)

$$i_s = i_d = \frac{U_s}{X}\sin\delta \tag{12}$$

where U_s expresses the output voltage of the inverter, U_g is the grid voltage, X means the reactance of the grid-connected transformer and connecting lines, and δ is the power angle of the system during operation.

Considering the voltage control effect, the following equations (2) and (11) can be obtained as

$$i_d = \frac{U_s}{X}\sin\delta = (u_{dc} - U_{dcref})(K_{pu} + \frac{K_{iu}}{s}) \tag{13}$$

Similar to the analysis of rotor dynamic characteristics, linearizing equation (13) near the steady-state operating point can be obtained as

$$sK\Delta\delta = (sK_{pu} + K_{iu})\Delta u_{dc} \tag{14}$$

where K is the structural parameter of the system and $K = U_s/\cos\delta$.

When input power variation is not considered, $\Delta i_{dc} = 0$. After linearizing equation (10), substitute it into equation (14) and eliminated Δu_{dc}, the dynamic model of DC capacitance of grid-connected inverter under DC voltage time scale can be written as

$$T_{Jc}(s)\frac{d\Delta\omega}{dt} = -T_{Dc}(s)\Delta\omega - T_{Sc}(s)\Delta\delta \tag{15}$$

where $T_{JC}(s)$, $T_{DC}(s)$, $T_{SC}(s)$ respectively represent equivalent inertia characteristics under DC capacitance control, damping characteristics, and synchronization characteristics [14]. $T_{JC}(s)$, $T_{DC}(s)$, $T_{SC}(s)$ are expressed as

$$\begin{cases} T_{Jc}(s) = CU_{dc}^2/S_B \\ T_{Dc}(s) = 1.5K_{pu}U_g \\ T_{Sc}(s) = 1.5K_{iu}U_g \end{cases} \tag{16}$$

Equation (16) shows that the dynamic characteristics of the capacitor can be described by equivalent parameters $T_{JC}(s)$, $T_{DC}(s)$ and $T_{SC}(s)$, which characterize the inertia, damping and synchronization effects of the system in the time scale of DC voltage. The equivalent inertia coefficient is related to capacitance and DC bus voltage level, the equivalent damping coefficient is related to voltage outer loop proportional control parameter and grid voltage level, and the equivalent synchronization coefficient is related to the integral control parameters of the voltage outer-loop and the standard value of the grid voltage. (The detailed derivation process of Equation (16) is given in the appendix).

C. INERTIA DAMPING CHARACTERISTICS OF D-PMSG GRID-CONNECTED SYSTEM

In the traditional power system dominated by synchronous generators, the grid frequency is closely related to the rotor speed. However, due to the existence of the intermediate DC link in the D-PMSG grid-connected power generation system, the mechanical process of the system rotor and the electromagnetic process on the AC side are connected, which makes the dynamic analysis of the system complicated. Referring to the traditional electric torque analysis method in power system, DC capacitor is taken as the equivalent rotor (referred to as 'static synchronous generator' in document [14], [15]), and the dynamic stability of the system is reflected by DC capacitor voltage. According to the analysis in sections 2.1 and 2.2, equivalent Phillips-Heffron models including virtual inertia control of the system can be respectively obtained as shown in Fig. 7 [11].

Fig. 4 shows that the dynamic characteristics of DC capacitor and synchronous generator in the D-PMSG grid-connected power generation system have certain similarities. The equivalent inertia, damping and synchronization coefficient of the system respectively represent the dynamic stability of the system from different angles. Note that due to the introduction of virtual inertia, the DC capacitor voltage is dynamically affected by the virtual inertia control as shown in the dashed box in Fig. 4. In order to analyze the influence of virtual inertia on multiple DC voltage time scales, the virtual inertia action channel is equivalently transformed into inertia, damping and synchronization effect paths, and the equivalent

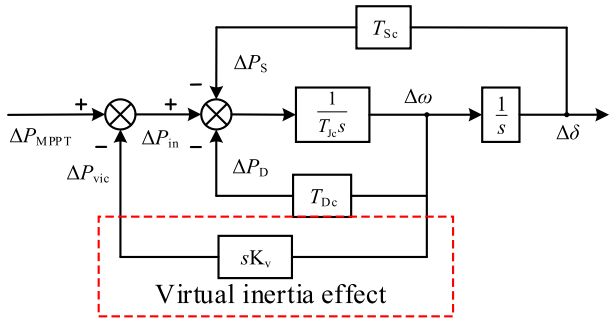

FIGURE 4. Equivalent Phillips-Heffron model for D-PMSG grid-connected power generation system.

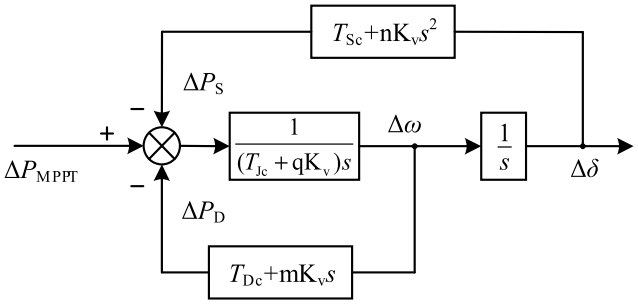

FIGURE 5. Equivalent Phillips-Heffron model for D-PMSG grid-connected power generation system.

Phillips-Heffron model of D-PMSG grid-connected power generation system is obtained again as shown in Fig. 5. In this figure, q, m and n respectively represent the acting coefficients of virtual inertia acting on inertia, damping and synchronization paths, and q+m+n=1.

The equivalent inertia, damping and synchronization parameters of the D-PMSG grid-connected power generation system under the virtual inertia control can be obtained from Fig. 5, respectively

$$\begin{cases} T_J(s) = T_{Jc}(s) + qK_v \\ T_D(s) = T_{Dc}(s) + mK_v s \\ T_S(s) = T_{Sc}(s) + nK_v s^2 \end{cases} \tag{17}$$

Equation (17) shows that the dynamic characteristics of the system can be described by equivalent parameters $T_J(s)$, $T_D(s)$, $T_S(s)$, which characterize the inertia, damping and synchronization effects of the system under the mechanical time scale of the wind turbine rotor and the time scale of DC voltage. Among them, the equivalent inertia coefficient is not only related to the capacitance and DC bus voltage level, but also related to the virtual inertia control parameters of the front stage. The equivalent damping coefficient is not only related to the proportional control parameter of the voltage outer loop and the grid voltage level value, but also related to the virtual inertia control parameter and the first derivative of the frequency change. The equivalent synchronization coefficient is not only related to the voltage outer loop integral control parameter and the grid voltage level value, but also related to the virtual inertia control parameter and the second derivative of power angle change.

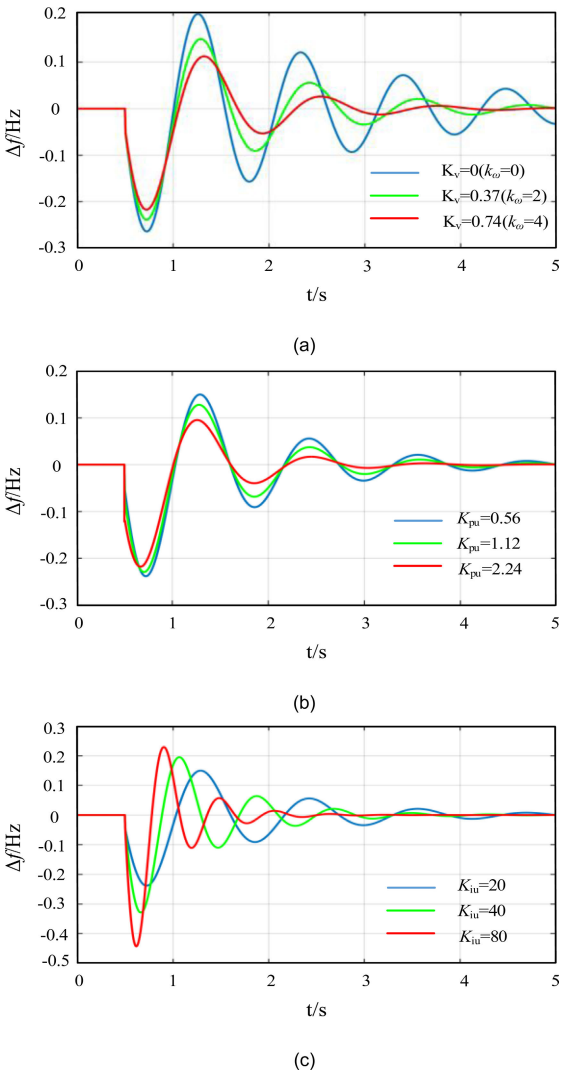

FIGURE 6. System frequency variation curve under the influence of different parameters. (a) the system frequency variation curve under the influence of K_v. (b) system frequency variation curve under the influence of K_{pu}. (c) the system frequency change curve under the influence of K_{iu}.

According to the system parameters in table 1, a D-PMSG equivalent Phillips-Heffron model as shown in Fig. 5 is established. Setting the system to generate a small power angle (about 5°) disturbance at 0.5s, the system frequency deviation curve can be obtained as shown in Fig. 6. The influence of the virtual inertia adjustment coefficient K_v on the system frequency curve can be obtained as shown in Fig. 6(a), which reflects the influence of the system equivalent inertia on the frequency dynamics [26]. In Fig. 6(b), the DC voltage control proportional coefficient K_{pu} on the system frequency curve. It reflects the effect of equivalent damping on the frequency dynamics of the system. In Fig. 6(c), the influence of the integral voltage coefficient K_{iu} of the graph on the system frequency curve reflects the influence of the equivalent synchronization effect of the system on the frequency dynamics.

It can be seen from Fig. 6 that the virtual inertia of the fan rotor has a great influence on the equivalent inertia of the system. It can also be found from equation (17) that the influence of virtual inertia coefficient on damping and synchronization is related to the first derivative of frequency change and the second derivative of power angle change. When the frequency changes little, it has little effect on it, so there can be p>m and p>n.

According to the above analysis, it can be seen that the main influence of damping is the amount of variation in the process of frequency change, and a larger inertia effect can alleviate the problem of large frequency variation. Damping mainly affects the magnitude of frequency variation in the process of frequency variation. Larger damping can reduce frequency deviation. The synchronization effect mainly affects the oscillation frequency in the process of frequency change. A larger synchronization coefficient can accelerate the frequency recovery, but it will also make change of the frequency overshoot too large.

IV. SIMULATION ANALYSIS AND RESULT VERIFICATION

A. SETTING OF SIMULATION PARAMETERS

In order to verify the correctness of the mechanism analysis of inertia damping characteristics of direct-drive wind power generation system and the influence law of parameters in this paper, a single machine infinite grid simulation model as shown in Fig. 1 is built on MATLAB/Simulink simulation platform. The output of the direct-drive wind turbine is connected to the power grid through a 0.69/10kV step-up transformer. The main parameter settings of the simulation system are shown in Table 1. On this basis, in order to verify the action law of equivalent parameters, the operating condition of the simulation system is set to generate power angle disturbance of about 10 at 13s.

TABLE 1. Main parameters of grid connected power generation system with direct drive wind.

Parameter	Quantity	Value and unit
S_B	System capacity	2/MW
U_g	Power voltage	10/kV
f	Grid frequency	50/Hz
U_0	Output voltage	690/V
U_{dc}	DC voltage	1200/V
K_{pu}	PI parameter	0.56
K_{Iu}	PI parameter	20
C	DC capacitor	0.12/F
p	Number of pole pairs	30
k_v	virtual inertia adjustment coefficien	0.37
k_w	modulation depth	2

B. ANALYSIS OF INFLUENCE LAW OF PARAMETERS

1) ANALYSIS OF INERTIA RESPONSE CHARACTERISTICS

As shown in Fig. 7, the output frequency curve of inverter and curve of DC bus voltage are respectively under disturbance. When the grid is disturbed, as system inertia effect of the virtual inertia control is enhanced, the output frequency of the inverter changes at the lowest point of the first swing and oscillation, then the anti-disturbance capability of the system frequency is also enhanced in Fig. 7 (a). The variation curve of the DC bus voltage is set out in Fig. 7(b). It can be noted from the figure that with the increase of the virtual inertia coefficient, fluctuation of the DC bus voltage increases. The more violent fluctuation of the DC bus voltage, the more kinetic energy released by the rotor and the greater the transient energy provided to the system.

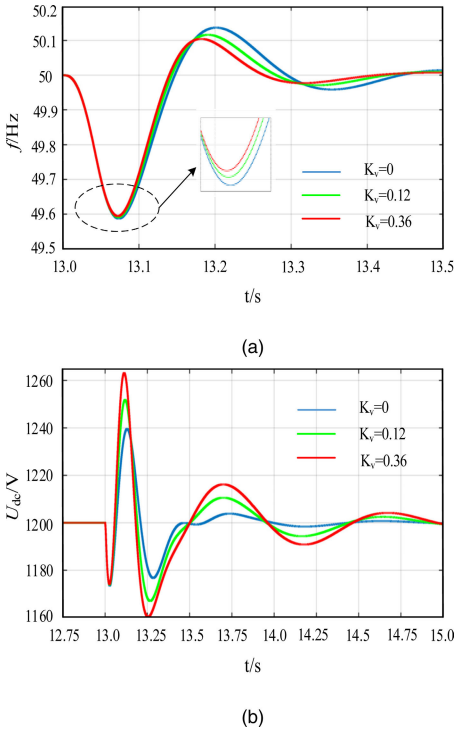

FIGURE 7. Influence analysis of equivalent inertia coefficient. (a) frequency variation curve of system. (b) capacitance-voltage change.

2) ANALYSIS OF DAMPING RESPONSE CHARACTERISTICS

As shown in Fig. 8, the output frequency curve of inverter and curve of DC bus voltage are respectively under disturbance. When the grid is disturbed, according to equation (17), the equivalent damping of the system builds up over the increase of the DC voltage proportional coefficient. As shown in Fig. 8(b), the smaller fluctuation of the DC voltage, the smaller the oscillation amplitude. Compared with Fig. 8(a), the frequency change of system is also improved.

3) CHARACTERISTIC ANALYSIS OF SYNCHRONIZATION EFFECT

As shown in Fig. 9, the output frequency curve of inverter and curve of DC bus voltage are respectively under disturbance. When the grid is disturbed, according to equation (17), the equivalent synchronization effect of the system grows at the increase of the DC voltage integral coefficient. As showing in Fig. 9(b), with the increase of the integration coefficient, the DC voltage oscillation period obviously changes, and the time to regain the steady state is shortened, but the

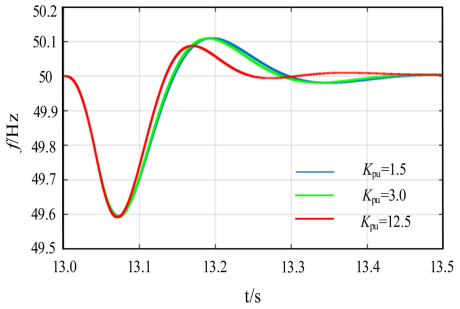

(a)

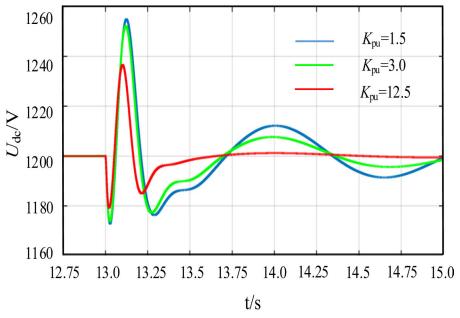

(b)

FIGURE 8. Influence analysis of equivalent damping coefficient. (a) system frequency variation curve. (b) capacitance-voltage change.

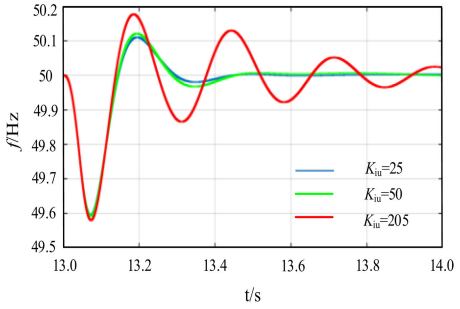

(a)

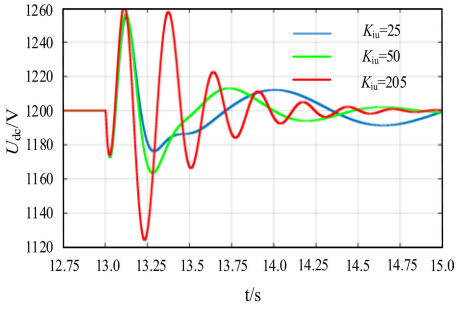

(b)

FIGURE 9. Influence analysis of equivalent synchronization coefficient. (a) the frequency variation curve of system. (b) capacitance-voltage change.

overshoot in the oscillation process obviously increases. The frequency changes the curve of the system corresponding to Fig. 9(a) also has a similar change trend.

V. CONCLUSION

In order to guarantee the correctness of the analysis of the inertia damping characteristics of the system under the control of virtual inertia. In this paper, the direct drive wind generation grid-connected system is used as the research object, so then the following conclusions are obtained:

1) With regard to the D-PMSG grid connected system, the control parameters, steady-state working points and structural parameters all have established influence on the inertia damping characteristics.

2) In terms of control parameters, the equivalent inertia coefficient of the system is centrally affected by the fictitious inertia coefficient K_V of the wind turbines; the equivalent damping coefficient is mainly influenced by the proportional control coefficient K_{pu} of the DC voltage; the equivalent synchronization coefficient is mainly affected by the integral control coefficient K_{iu} of the DC voltage.

3) The dynamic performance of the system is affected by equivalent inertia, damping and synchronization coefficient. Compared with the steady-state action spot and structural parameters of the system, it is the simplest way to improve the dynamic performance of the system by changing the control parameters.

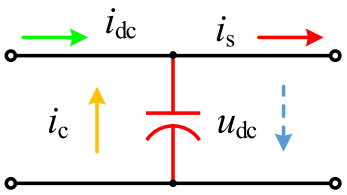

FIGURE 10. Schematic diagram of charging and discharging of DC bus capacitor.

APPENDIX

As shown in Fig. 10, the charging and discharging diagram of DC bus capacitor is shown. i_{dc}, i_c, i_s and u_{dc} in the diagram are input current, capacitor current, output current and capacitor voltage respectively.

According to the charging and discharging law of the capacitor, the expression of capacitance current i_c can be written as

$$i_c = C_{dc}\frac{du_{dc}}{dt} = i_{dc} - i_s \tag{A.1}$$

Reformulated the current i_c in formula (A.1) as

$$i_c = C_{dc}\frac{du_{dc}}{dt} = \frac{\frac{1}{2}C_{dc}U_{dc}^2}{\frac{1}{2}C_{dc}U_{dc}^2}C\frac{du_{dc}}{dt} = \frac{2E_k}{U_{dc}^2}\frac{du_{dc}}{dt} \tag{A.2}$$

where E_k is the energy stored by the capacitor. Selecting the reference voltage as the DC bus voltage U_{dc} and the rated capacity S_B of the power selection system, the reference current I_B can be expressed as

$$I_B = \frac{S_B}{U_{dc}} = \frac{P_B}{U_{dc}} \tag{A.3}$$

Combining equation (A.1) and dividing the two sides of the equation by the current reference I_B, it can be expressed as

$$i_c^* = \frac{i_c}{I_B} = \frac{2E_k}{I_B U_{dc}} \frac{d(\frac{u_{dc}}{U_{dc}})}{dt} = \frac{2E_k}{P_B} \frac{du_{dc}^*}{dt} = \frac{i_{dc}}{I_B} - \frac{i_s}{I_B} = i_{dc}^* - i_s^* \tag{A.4}$$

Referring to the definition of inertia time constant of power system, the inertia time constant of capacitance can be defined as

$$T_{Jc}(s) = \frac{CU_{dc}^2}{S_B} == \frac{CU_{dc}^2}{P_B} \tag{A.5}$$

Therefore, the formula (A.1) can be reformulated as

$$T_{Jc} \frac{du_{dc}^*}{dt} = i_{dc}^* - i_s^* \tag{A.6}$$

In order to facilitate analysis, if equation (A.6) is reformulated as a power expression, it can be written as

$$T_{Jc} \frac{du_{dc}^*}{dt} = i_{dc}^* - i_s^* = \frac{P_{dc}^*}{u_{dc}^*} - \frac{P_s^*}{u_{dc}^*} \tag{A.7}$$

Under the control of the voltage outer loop, the change is small, which can be considered as approximately 1, then it can be written as

$$T_{Jc} \frac{du_{dc}^*}{dt} = P_{dc}^* - P_s^* \tag{A.8}$$

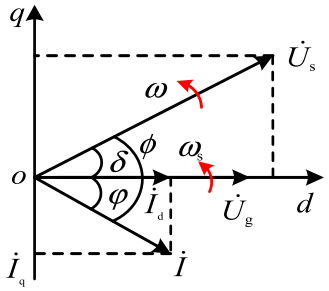

FIGURE 11. Voltage and current vector diagram.

The vector diagram when grid voltage orientation is adopted for grid-connected current control is shown in Fig. 11. According to the diagram, the expression of grid-connected current can be obtained as (ignoring the current component of filter capacitor)

$$i_s = i_d = \frac{U_s}{X} \sin\delta \tag{A.9}$$

Considering the voltage control effect, from equation (A.9), it can be obtained as

$$i_d = \frac{U_s}{X} \sin\delta = (u_{dc} - U_{dcref})(K_{pu} + \frac{K_{iu}}{s}) \tag{A.10}$$

Equation (A.10) is linearized near a steady-state operating point, it can be expressed as

$$sK\Delta\delta = (sK_{pu} + K_{iu})\Delta u_{dc} \tag{A.11}$$

where K is the structural parameter of the system, and $K = U_s/\cos\delta_0$. What happens when input power changes are not considered $\Delta i_{dc} = 0$, equation (8) is linearized $s\Delta\delta = \Delta\omega$ to consider equation (A.11) and cancel Δu_{dc} can obtain. The dynamic model of DC capacitance of the grid-connected inverter in DC voltage time scale can be expressed as

$$T_{Jc}(s)\frac{d\Delta\omega}{dt} = -T_{Dc}(s)\Delta\omega - T_{Sc}(s)\Delta\delta \tag{A.12}$$

Among them

$$\begin{cases} T_{Jc}(s) = CU_{dc}^2/S_B \\ T_{Dc}(s) = 1.5K_{pu}U_g \\ T_{Sc}(s) = 1.5K_{iu}U_g \end{cases} \tag{A.13}$$

REFERENCES

[1] W. Gang, S. Qiaoming, C. Zhiyong, F. Lijun, and W. You, "A coordinated strategy of virtual inertia control of wind turbine and governor control of conventional generator," *Power Syst. Technol.*, vol. 10, no. 39, pp. 2794–2801, 2015.

[2] Z. Xiaoxin, L. Zongxiang, L. Yingmei, and C. Shuyong, "Development models and key technologies of future grid in China," *Proc. CSEE*, vol. 29, no. 34, pp. 4999–5008, 2014.

[3] T. Xisheng, F. Miao, Z. Qi, H. He, T. Wu, and S. Li, "Survey on frequency control of wind power," *Proc. CSEE*, vol. 25, no. 34, pp. 4304–4314, 2014.

[4] X. Yuan, S. Cheng, and J. Hu, "Multi-time scale voltage and power angle dynamics in power electronics dominated large power systems," *Proc. CSEE*, vol. 19, no. 36, pp. 5145–5154, 2016.

[5] Z. Qingchang, "Virtual synchronous machines and autonomous power systems," *Proc. CSEE*, vol. 2, no. 37, pp. 336–349, 2017.

[6] T. Shintai, Y. Miura, and T. Ise, "Oscillation damping of a distributed generator using a virtual synchronous generator," *IEEE Trans. Power Del.*, vol. 29, no. 2, pp. 668–676, Apr. 2014.

[7] H. Bevrani, T. Ise, and Y. Miura, "Virtual synchronous generators: A survey and new perspectives," *Int. J. Electr. Power Energy Syst.*, vol. 54, pp. 244–254, Jan. 2014.

[8] Y. Cai, Z. Li, and X. Cai, "Optimal inertia reserve and inertia control strategy for wind farms," *Energies*, vol. 13, no. 5, p. 1067, Mar. 2020.

[9] L. Holdsworth, J. B. Ekanayake, and N. Jenkins, "Power system frequency response from fixed speed and doubly fed induction generator-based wind turbines," *Wind Energy*, vol. 7, no. 1, pp. 21–35, Jan. 2004.

[10] H. Jiafa, M. Song, Z. Lan, and L. Huang, "A virtual inertia coordinated control scheme of PMSG-based wind turbines in weak grids," *Autom. Electr. Power Syst.*, vol. 42, no. 9, pp. 83–90, 2018.

[11] J. Fang, H. Li, Y. Tang, and F. Blaabjerg, "Distributed power system virtual inertia implemented by grid-connected power converters," *IEEE Trans. Power Electron.*, vol. 33, no. 10, pp. 8488–8499, Oct. 2018.

[12] J. Fang, H. Li, Y. Tang, and F. Blaabjerg, "On the inertia of future more-electronics power systems," *IEEE J. Emerg. Sel. Topics Power Electron.*, vol. 7, no. 4, pp. 2130–2146, Dec. 2019.

[13] L. Huang, H. Xin, Z. Wang, K. Wu, H. Wang, J. Hu, and C. Lu, "A virtual synchronous control for voltage-source converters utilizing dynamics of DC-link capacitor to realize self-synchronization," *IEEE J. Emerg. Sel. Topics Power Electron.*, vol. 5, no. 4, pp. 1565–1577, Dec. 2017.

[14] L. Xiong, F. Zhuo, F. Wang, X. Liu, Y. Chen, M. Zhu, and H. Yi, "Static synchronous generator model: A new perspective to investigate dynamic characteristics and stability issues of grid-tied PWM inverter," *IEEE Trans. Power Electron.*, vol. 31, no. 9, pp. 6264–6280, Sep. 2016.

[15] X. Liancheng, X. Liansong, and K. Zhiliang, "Analysis for dynamic characteristics of grid-tied energy storage system with droop control," *J. Xi'an Jiaotong Univ.*, vol. 51, no. 12, pp. 1–9, 2018.

[16] Y. Hao and Y. Xiao, "Modeling and characteristic analysis of grid-connected VSCs based on amplitude-phase motion equation method for power system transient process study in DC-link voltage control timescale," *Proc. CSEE*, vol. 23, no. 38, pp. 6882–6892, 2018.

[17] Y. Qian, X. Yuan, and M. Zhao, "Analysis of voltage control interactions and dynamic voltage stability in multiple wind farms," in *Proc. IEEE Power Energy Soc. Gen. Meeting (PESGM)*, Jul. 2016, pp. 1–5.

[18] Y. Huang, X. Yuan, and J. Hu, "Effect of reactive power control on stability of DC-link voltage control in VSC connected to weak grid 2014," in *Proc. IEEE PES Gen. Meeting Conf. Expo.*, 2014, pp. 1–5.
[19] J. Ying, X. Yuan, J. Hu, and W. He, "Impact of inertia control of DFIG-based WT on electromechanical oscillation damping of SG," *IEEE Trans. Power Syst.*, vol. 33, no. 3, pp. 3450–3459, May 2018.
[20] J. Ying, X. Yuan, and J. Hu, "Inertia characteristic of DFIG-based WT under transient control and its impact on the first-swing stability of SGs," *IEEE Trans. Energy Convers.*, vol. 32, no. 4, pp. 1502–1511, Dec. 2017.
[21] P. Kundur, *Power System Stability and Control*. New York, NY, USA: McGraw-Hill, 1994.
[22] K. Liu, Y. Qu, H.-M. Kim, and H. Song, "Avoiding frequency second dip in power unreserved control during wind power rotational speed recovery," *IEEE Trans. Power Syst.*, vol. 33, no. 3, pp. 3097–3106, May 2018.
[23] B. K. Poolla, S. Bolognani, and F. Dorfler, "Optimal placement of virtual inertia in power grids," *IEEE Trans. Autom. Control*, vol. 62, no. 12, pp. 6209–6220, Dec. 2017.
[24] A. Sangwongwanich, Y. Yang, F. Blaabjerg, and H. Wang, "Benchmarking of constant power generation strategies for single-phase grid-connected photovoltaic systems," *IEEE Trans. Ind. Appl.*, vol. 54, no. 1, pp. 447–457, Jan. 2018.
[25] W. Wu, Y. Chen, A. Luo, L. Zhou, X. Zhou, L. Yang, Y. Dong, and J. M. Guerrero, "A virtual inertia control strategy for DC microgrids analogized with virtual synchronous machines," *IEEE Trans. Ind. Electron.*, vol. 64, no. 7, pp. 6005–6016, Jul. 2017.
[26] F. Yuan, Y. Wang, X. Zhang, and Y. L. Luo, "Analysis and integrated control of inertia and primary frequency regulation for variable speed wind turbines," *Proc. CSEE*, vol. 34, no. 24, pp. 4706–4716, 2014.
[27] H. Wu, X. Ruan, D. Yang, X. Chen, W. Zhao, Z. Lv, and Q.-C. Zhong, "Small-signal modeling and parameters design for virtual synchronous generators," *IEEE Trans. Ind. Electron.*, vol. 63, no. 7, pp. 4292–4303, Jul. 2016.
[28] J. F. Conroy and R. Watson, "Frequency response capability of full converter wind turbine generators in comparison to conventional generation," *IEEE Trans. Power Syst.*, vol. 23, no. 2, pp. 649–656, May 2008.
[29] L. Miao, J. Wen, H. Xie, C. Yue, and W.-J. Lee, "Coordinated control strategy of wind turbine generator and energy storage equipment for frequency support," *IEEE Trans. Ind. Appl.*, vol. 51, no. 4, pp. 2732–2742, Jul. 2015.
[30] X. Meng, J. Liu, and Z. Liu, "A generalized droop control for grid-supporting inverter based on comparison between traditional droop control and virtual synchronous generator control," *IEEE Trans. Power Electron.*, vol. 34, no. 6, pp. 5416–5438, Sep. 2019.
[31] D. Xu, Q. Wu, B. Zhou, C. Li, L. Bai, and S. Huang, "Distributed multi-energy operation of coupled electricity, heating, and natural gas networks," *IEEE Trans. Sustain. Energy*, vol. 11, no. 4, pp. 2457–2469, Oct. 2020.

SHENGQING LI received the B.S. and M.S. degrees in physics from Hunan Normal University and the Ph.D. degree in power system and automation from Hunan University, Hunan, China. Since 2001, he has been teaching and researching with the Hunan University of Technology, where he is currently a Professor and engaged in research work on power supply quality control of distribution network and power electronic system control. He is also a member of the Provincial Electro-technical Society and a Vice Chairman of the Provincial Theoretical Electro-technical Committee.

YU JIANG was born in Shanxi, China, in 1996. She is currently pursuing the M.S. degree in power electronics and power drives with the Hunan University of Technology. Her main research interest includes wind power grid connection.

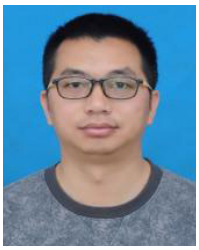

BALING FANG (Member, IEEE) was born in Hunan, China, in 1980. He received the M.B.A. degree from Jilin University, Jilin, China, in 2009, and the Ph.D. degree in electrical engineering from Hunan University, Changsha, China, in 2017. He is currently an Associate Professor with the College of Electrical and Information Engineering, Hunan University of Technology, Zhuzhou, China. His research interests include smart grid operation and planning, renewable energy generation, and cloud computing.

CHENYANG WANG is currently pursuing the M.S. degree in power electronics and power drives with the Hunan University of Technology. His research interest includes control strategy of three-phase high-frequency chain matrix converter.